Research on Green Wave Guidance Strategy Under Cross-Network Collaboration Architecture

Lingqiu Zeng[1,2] and Yuqiao Liu[1] and Qingwen Han[1] and Jianmei Lei[2*]
and Yufei Yan[1] and Lei Ye[1] and Ruilong Yang[1]

***Abstract*—Green wave guidance is an important application in intelligent transportation. This paper proposes a green wave guidance strategy based on cross-network collaboration. First, a cross-network collaboration framework is introduced to optimize multi-intersection green wave guidance, incorporating an improved Ising model for road pass-through rate assessment. Then, an improved ant colony algorithm based on road pass-through rate distribution is developed to generate vehicle trajectory guidance and speed recommendations, with a dynamic trajectory update strategy to enhance information usability. Experimental results show that this method effectively evaluates traffic conditions and improves vehicle passage efficiency.**

***Index Terms*—Cross-network collaboration, Ising model, Road pass-through rate, Green wave guidance strategy**

I. Introduction

With the rapid increase in vehicle ownership, traffic congestion has become a global problem. Drivers dream of hitting every green light, thus minimizing vehicle travel time. The green wave system, which provides reasonable driving suggestions to avoid encountering red lights, is considered an effective solution to alleviate traffic congestion and reduce energy consumption [1].

Arterial traffic signal optimization is an effective way to maximize the green wave band [2]. There is no doubt that such a methodology could schedule traffic flow reasonably, but it lacks service capability for individual drivers. In practice, drivers could actively avoid red lights by adjusting cruising velocity and selecting an optimal trajectory. The only problem is how to provide reliable and valid driving guidance.

Vehicle-Road-Cloud Integrated System (VRCIS) [3] not only could collect real-time road and vehicle information, but also provide driving suggestions and control service relying on both V2X technologies and powerful computation resources. As early as 2011, Yang et al. [4] proposed a novel speed guidance strategy on the basis of bidirectional communication between vehicles and infrastructures in VII system. Then, researchers have proposed various vehicle speed guidance strategies to instruct drivers to adjust driving behavior according to real-time traffic features and traffic signal light phase [5], which are obtained via V2X data exchange.

[1]Chongqing University, Chongqing, 400044, China. `zenglq@cqu.edu.cn, 202514131070t@stu.cqu.edu.cn, hqw@cqu.edu.cn,202112131092@cqu.edu.cn, Yelei@cqu.edu.cn, yangrl@cqu.edu.cn`
[2]State Key Laboratory of Intelligent Vehicle Safety Technology, Chongqing, 400020, China. `leijianmei@caeri.com.cn`
*corresponding author

IMT2020(5G) V2X Working Group and CCSA (China Communication Standard Association) initiated Cross-Network Collaboration (CNC) research projects, which aim to combine the advantages of both Uu (4G, 5G) and PC5, thus providing enhanced traffic efficiency service. As one of the important applications of CNC architecture, Multi-intersection Green Wave Guidance (MiGWG) was selected as a key issue of the CNC project.

CNC-based application research includes two aspects of content: CNC data exchange procedure and application-oriented algorithm optimization. CNC data exchange procedure and corresponding interface are defined on the basis of works on CCSA (China Communication Standard Association) YDT 3977-2021. In this paper, we focus on MiGWG application-oriented algorithm optimization, specifically, MiGWG-oriented driving trajectory optimization.

CNC architecture makes it possible to collect on-road vehicles' cruising states information and traffic light phase, which are used to provide MiGWG service. Obviously, the CNC-oriented MiGWG strategy not only considers real-time traffic-based phase matrix adjustment [6], but also V2X information for collaborative control [7]. Thus, in this paper, an index, the pass-through rate of the road section, which combines both real-time traffic feature and light phase, is defined as an impact of MiGWG guidance generation, and calculated by the edge V2X server. Therefore, the rationality of the learning model deployed on the edge side has a profound impact on the pass-through rate. The selection of the edge side learning model should consider both efficiency and accuracy. In general, Machine-learning-based methods, e.g., Support Vector Machine (SVM), Residual Neural Networks (ResNet), are used to analyze traffic flow, but hardly match the real-time feature of MiGWG. [8] proposed an optimized GRU-based traffic flow prediction model that enhances temporal dependency learning. On the other hand, attention-based networks perform well in time series prediction [8]. In particular, the Gated Recurrent Unit (GRU) provides a more computationally efficient alternative for sequential modeling. By simplifying the gating structure of LSTM while retaining its ability to alleviate gradient vanishing, GRU achieves faster training and lower inference cost with fewer parameters [9], making it suitable for streaming traffic data processing. Moreover, transformer architecture, which replaces recurrent operations with self-attention [10], is effective in capturing long-range temporal correlations and complex global patterns, and is beneficial for accuracy improvement. Therefore, this paper proposes a spatiotemporal prediction model that integrates GRU with a transformer-based attention mechanism to balance real-time performance and accuracy, enabling low-latency updates for streaming data.

In the field of trajectory planning, graph search algorithms [11] are commonly applied. [12] demonstrated the successful use of the Dijkstra algorithm to enable an autonomous vehicle to complete a 150-mile off-road challenge within a very short time. In [13], the A* algorithm was employed for trajectory planning, taking into account the vehicle's contour to generate safer driving routes and enhance travel efficiency. Neural networks and nature-inspired algorithms have also become research hotspots in this domain. [14] proposed a method combining Particle Swarm Optimization with fuzzy neural networks to overcome the limitations of traditional fuzzy neural networks in terms of computational complexity and convergence speed, thus supporting intelligent vehicle trajectory planning. [15] presented an improved Rapidly Exploring Random Tree (RRT) algorithm, which is applicable to vehicle trajectory planning and can enhance driving efficiency. Building on these works, we propose a MiGWG strategy based on Ant Colony Optimization (ACO), integrated within a cross-network collaborative framework. It incorporates real-time pass-through rate evaluation of the road to enable multi-intersection green wave passage for vehicles.

II. PRELMINARIES

In this section, the basic CNC system architecture that provides MiGWG service is introduced, while the corresponding data set is explained.

A. System Architecture

CNC system architecture for MiGWG service is shown in Fig. 1.

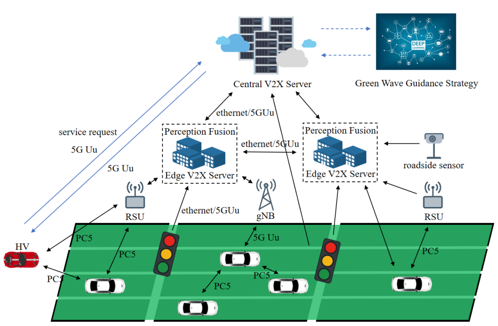

Fig. 1: CNC system architecture for MiGWG service.

The MiGWG service strategy is constructed on the basis of the pass-through rate, which is evaluated at edge V2X servers. As shown in Fig.1, edge V2X servers collect real-time traffic status information, e.g., regional vehicle density, vehicle cruising speed (including maximum speed, minimum speed, average speed, etc.), vehicle driving trajectory, driving intention information (target road information of the service object vehicle planning), etc., via LTE V2X/5Guu, and calculate pass-through rate of corresponding road sections. Then, according to the cruising status of the host vehicle (HV), the multi-intersection traffic light phase scheme, and the processing results of the roadside perception & processing units, the central V2X servers should generate MiGWG suggestion information, e.g., cruising speed, cruising lane, mesoscopic trajectory, etc.

The relevant roles are described as follows.

1) Vehicle end users: Service users who send a MiGWG service request message to the V2X server, which generates corresponding MiGWG suggestion information. Vehicle end users should be equipped with a communication module, e.g., LTE V2X module, 5G Uu module.

2) Telecommunications operators: Telecommunications operators deploy roadside facilities, e.g., LTEV2V RSUs, gNBs, and edge/central V2X servers. Telecommunications operators provide communication and computation resources for the MiGWG service.

3) Service providers: Internet companies, transportation service companies, and telecommunications operators could act as service providers. Service providers generate corresponding MiGWG service information and compete for customers.

B. Raw Data Set

The raw data set, which was provided by the ICV demonstration zone, Yongchuan, Chongqing, China, is used to train the model for pass-through rate evaluation. The road section, which includes 300 meters of road, 1 intersection, and 1 T section, is shown in Fig. 2. The trajectories of the vehicles on the road are collected by roadside Lidars, which are deployed at the points of the red triangle in Fig. 2.

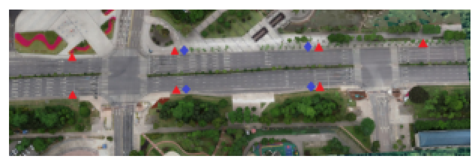

Fig. 2: Road section of raw data set.

The Lidar data piece includes 13 indexes, e.g., vehicle type, identification number, longitude/ latitude, cruising speed, heading, etc. 90 days Lidar data set, which includes 550746 data pieces, is used.

III. PROPOSED METHOD

The edge/central V2X servers collect real-time regional traffic features to generate service information based on pass-through rate. Then, two issues are involved: pass-through rate generation and MiGWG trajectory generation.

A. Multi-intersection pass-through rate generation

The model architecture for multi-intersection pass-through rate generation consists of the Sequence Perception Module and Feature Enhancement Module, as illustrated in Fig. 3.

1) Multi-intersection pass-through rate: For Lidar data, statistical kinematic features are extracted from all observed vehicle trajectories to construct a trajectory feature matrix $V_t \in \mathbb{R}^{G \times d_v}$, where G denotes the number of spatial grids and d_v represents the dimensionality of vehicle dynamic attributes, such as position, speed, and acceleration. It is taken into account to derive the vehicle pass status s_i, which is defined as follows:

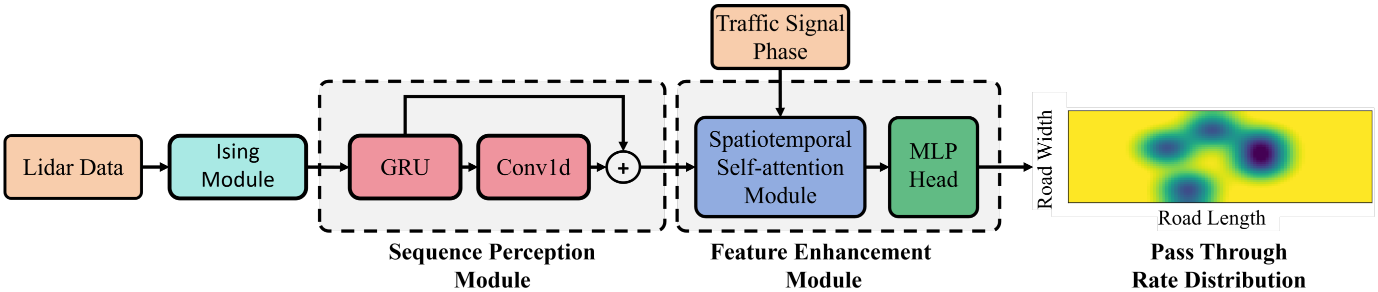

Fig. 3: Model architecture.

$$s_i = \begin{cases} +1 & \text{if } v_{\text{current}} \cdot (nT + t_{\text{green\_res}}) \\ & +0.5 \cdot a_{\text{acc}}^{\max} \cdot (nT + t_{\text{green\_res}})^2 \geq d \\ & \text{and } v_{\text{current}} + a_{\text{acc}}^{\max} \cdot (nT + t_{\text{green\_res}}) \leq V_{\max} \\ & \text{and state} = 1 \\ +1 & \text{if } v_{\text{current}} \cdot (nT + t_{\text{green\_res}}) \geq d \text{ and state} = 1 \\ +1 & \text{if } v_{\text{current}} + a_{\text{acc}}^{\max} \cdot (t_{\text{red\_res}} + t_{\text{green}} + nT) \leq V_{\max} \\ & \text{and } v_{\text{current}} \cdot (t_{\text{red\_res}} + t_{\text{green}} + nT) \\ & +0.5 \cdot a_{\text{acc}}^{\max} \cdot (t_{\text{red\_res}} + t_{\text{green}} + nT)^2 \geq d \\ & \text{and state} = 0 \\ 0 & \text{otherwise} \end{cases} \tag{1}$$

$v_{current}$ is the vehicle's current speed. T is the traffic light cycle. d is the distance between the vehicle and the stop line. n is the number of intersections. $a_{\text{acc}}^{\max}$ is the maximum acceleration. $t_{\text{green\_res}}$ is the remaining time of the green light. $t_{\text{red\_res}}$ is the remaining time of the red light. t_{green} is the duration of the green light phase. $state$ is the status of the traffic light, where 1 is the green light and 0 is the red light.

As discussed in [16], the Ising model was used to evaluate the level of road hazard. Considering a multi-intersection scene, in this paper, the vehicle pass status s_i is introduced into the Ising model, and the overall pass-through rate of a specific road section is defined as:

$$\begin{aligned} H_w &= \frac{1}{N} \sum_i H_{\nu i} \\ H_{\nu i} &= \sum_{<i,j>} J_{i,j} s_i s_j + h(t) \sum_i s_i \end{aligned} \tag{2}$$

Where H_w is the overall pass-through rate of the road section; $H_{\nu i}$ represents the pass-through rate of vehicle i; N is the vehicle's number in the green wave area; s_i is the pass status of vehicle i; J is the inter-relationship between vehicle i and j; $h(t)$ is the external condition.

To further consider spatial constraints, the road section is divided into discrete grids, each grid accommodating at most one vehicle (larger vehicles occupy multiple grids). The pass status of the grid i is defined as follows:

$$s_{grid_i} = \begin{cases} s_i & if\ there\ is\ a\ vehicle\ in\ the\ grid \\ s_{road} & if\ there\ is\ no\ vehicle\ in\ the\ grid \end{cases} \tag{3}$$

Then the pass-through rate of the grid i at time t is defined as:

$$H_{i,t} = -J \sum_j s_{grid_i} s_j - h(t) \sum_i s_{grid_i} \tag{4}$$

Note that in CNC architecture, RSUs acquire road-vehicle information via PC5. The RSUs and the traffic light phase control unit then transmit their respective data to the edge V2X server, which estimates the road pass through rate based on these inputs. The edge V2X server evaluation results are subsequently forwarded to the central V2X server via Uu.

2) Sequence perception module: After the Ising Module, each spatial grid i at time t is represented by a pass-through feature $H_{i,t}$. The green-wave corridor is discretized into G ordered grids, which form the traffic state vector:

$$H_t = [H_{1,t}, H_{1,t}, ..., H_{G,t}] \in \mathbb{R}^G \tag{5}$$

To capture short-term temporal evolution while preserving grid-wise independence, a gated recurrent unit (GRU) processes the historical sequence of each grid over the past T time steps, producing $GRU(H_{i,t-T+1:t})$.

After processing all grids, the temporal encoding result at time t forms a feature map H_t^{gru}. To further refine local temporal patterns and suppress noise from instantaneous fluctuations, a one-dimensional convolution (Conv1d) is applied over H_t^{gru}, generating $\tilde{H}_t = Conv1d(H_t^{gru})$. The convolution output is then concatenated with the original GRU features through a residual connection, forming the final grid-level embedding $Z_t = Concat(H_t^{gru}, \tilde{H}_t)$, which serves as input to the subsequent feature enhancement module.

3) Feature enhancement module: To further integrate heterogeneous multi-source traffic information and capture long-range spatial dependencies among distant grids, the feature enhancement module is introduced, as illustrated in Fig. 4

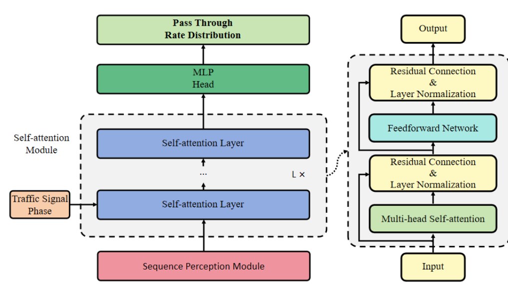

Fig. 4: Feature enhancement module.

The module consists of $L = 4$ stacked layers. Each layer contains a Multi-Head Self-Attention (MHSA) module and a Feed-Forward Network (FFN), both followed by residual connection and layer normalization. The MHSA employs 8 attention heads to capture diverse long-range spatial dependencies among grids. The position-wise FFN then performs the nonlinear feature transformation independently for each grid.

In urban traffic systems, vehicle movements are not only governed by local traffic states but also strongly regulated by traffic signal control. To incorporate this control mechanism into spatial dependency modeling, traffic signal phase information is introduced as an additional modality. The phase information of the traffic signal is encoded as a signal feature matrix $S_t \in \mathbb{R}^{G \times d_s}$,where d_s includes phase-related attributes such as the phase index and the remaining green time.

A linear embedding layer is employed to project heterogeneous features into a unified latent space. Z_t and S_t are transformed as:

$$\begin{aligned} E_{z,t} &= Z_t W_z + b_z \\ E_{sig,t} &= S_t W_{sig} + b_{sig} \end{aligned} \tag{6}$$

where W_z, W_{sig} are learnable projection matrices and b_z, b_{sig} are bias vectors. The embedded features are concatenated along the channel dimension to form a fused representation:

$$X_t = Concat(E_{z,t}, E_{sig,t}) \tag{7}$$

The MHSA employs a scaled dot-product mechanism to compute the interaction weight between any pair of spatial grids, allowing each grid to selectively aggregate information from other grids. This enables the model to capture long-range traffic dependencies. Following the attention block, the FFN applies a two-layer linear transformation with a non-linear activation independently to each grid, performing deep feature extraction and non-linear mapping on the fused vehicle trajectory and traffic signal features. For the l-th layer, this process can be summarized as follows:

$$\begin{aligned} \tilde{X}_t^{(l)} &= LayerNorm(X_t^{(l-1)} + MHSA(X_t^{(l-1)})) \\ X_t^{(l)} &= LayerNorm(\tilde{X}_t^{(l)} + FFN(\tilde{X}_t^{(l)})) \end{aligned} \tag{8}$$

After L stacked layers, the transformer encoder outputs the globally enhanced representation $X_t^{(l)}$. The feature corresponding to grid i at time t is denoted as x_i^t, then the multilayer perceptron (MLP) head maps each transformed token to a scalar value representing the predicted pass-through probability:

$$\hat{p}_{i,t} = \sigma(W_p x_i^t + b_p) \tag{9}$$

where, W_p and b_p are the weight matrix and the bias vector of the MLP, respectively, and $\sigma(\cdot)$ is the sigmoid function that constrains the output to the range from zero to one.

By collecting the predicted pass-through rates of all grids in the green-wave area, we obtain the pass-through rate distribution at time t:

$$\hat{P}_t = [\hat{p}_{1,t}, \hat{p}_{2,t}, ..., \hat{p}_{G,t}] \in \mathbb{R}^G \tag{10}$$

The Mean Squared Error(MSE) loss is adopted to quantify the discrepancy between the predicted pass-through rate and the ground-truth value. The loss function is defined as:

$$\mathcal{L}_{MSE} = \frac{1}{TG} \sum_{t=1}^{T} \sum_{i=1}^{G} (\hat{p}_{i,t} - p_{i,t})^2 \tag{11}$$

The aforementioned Lidar dataset was used for training. Training performance is shown in Fig. 5. Training and validation losses decrease steadily and eventually stabilize.

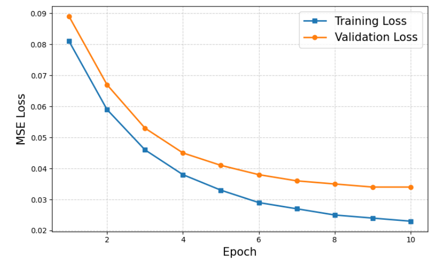

Fig. 5: Loss curve.

B. MiGWG Trajectory Planning

1) Trajectory planning algorithm: In this paper, the ant colony optimization(ACO) is applied to vehicle trajectory planning, using grids as basic search units.

ACO is to simulate the cooperative foraging behavior of ants, where indirect communication via pheromone trails enables the colony to collectively discover optimal paths. During the search process, each ant selects its next movement based on the current pheromone intensity and heuristic information associated with candidate paths. This decision-making process can be formally described using a probabilistic model.

Specifically, the path selection probability that an ant moves from grid i to grid j at time t, denoted as $p_{ij}^k(t)$, is determined as a function of the pheromone concentration and the corresponding heuristic desirability. The mathematical formulation is given as follows:

$$p_{ij}^k(t) = \begin{cases} \frac{C_{ij} \cdot [\tau_j(t)]^\alpha \cdot [\eta_j(t)]^\beta}{\sum_{s \in \Omega_k} [\tau_s(t)]^\alpha \cdot [\eta_s(t)]^\beta} & j \in \Omega_k \\ 0 & otherwise \end{cases} \tag{12}$$

Where C_{ij} is the speed constraint; $\tau_j(t)$ is the pheromone concentration on the grid j at time t; α is the pheromone concentration importance factor; $\eta_j(t)$ is the road pass-through rate heuristic information; β is the importance factor of the pass-through rate heuristic information; Ω_k is the set of feasible grids for the ants k to follow next.

The heuristic information $\eta_j(t)$ for the road pass-through rate is defined as follows:

$$\eta_j(t) = \lambda_1 e^{\frac{1}{n} \sum_{m=T}^{T+n} \hat{p}_{j,m}} \tag{13}$$

λ_1 is the weight coefficient and $\hat{p}_{j,m}$ is the road pass-through rate of the grid j at time m ; n is the number of future time steps.

2) Dynamic MiGWG Strategy Generation Method: The aforementioned ACO can only perform static trajectory planning and cannot be applied to dynamic scenarios. Therefore, this paper introduces a dynamic trajectory update strategy.

Long-distance trajectory planning increases computational complexity. Local trajectory planning is adopted. Each trajectory is generated within a defined search region. This enables the real-time generation of locally optimal solutions and ensures the continuous provision of trajectories. The search interval W_k is defined as:

$$W_k = [p_{start}, p_{end} + \Delta l] \tag{14}$$

where p_{start} and p_{end} denote the start and end positions of the interval, and Δl represents the length of the interval.

Then the path selection probability is updated as:

$$p_{ij}^k(t, W_k) = \begin{cases} \frac{C_{ij} \cdot [\tau_j(t,W_k)]^\alpha \cdot [\eta_j(t,W_k)]^\beta}{\sum_{s \in \Omega_k} [\tau_s(t,W_k)]^\alpha \cdot [\eta_s(t,W_k)]^\beta} & j \in \Omega_k \\ 0 & otherwise \end{cases} \tag{15}$$

The path selection probability is dynamically adjusted according to both pheromone intensity and heuristic value. Since the feasible search domain is restricted to the local region Ω_k, ants only explore nodes within the current interval, which significantly accelerates convergence while maintaining solution quality. After each local optimization cycle pheromone values are updated to reinforce high-quality trajectory segments, forming a dynamic trajectory update process.

IV. Experiments

A. Simulation Experimental Design

NS-3 and SUMO are used for collaborative simulation. The platform parameters are set according to the actual road conditions, as shown in table I and table II.

TABLE I: The parameter setting of the SUMO platform

SUMO platform parameters	Value
Lane length	3000m
Number of lanes	4
Lane width	3.5m
Number of vehicles	50
Number of traffic signals	5
Traffic signal cycle	90s
Green light duration of traffic signals	40s
Vehicle speed	20km/h - 60km/h

TABLE II: The parameter setting of the NS3 platform

Parameter Name	Value
Number of vehicle nodes	50
Number of RSUs	5
Number of gNBs	2
Number of MEC nodes	5
Number of cloud nodes	1
Number of traffic signal nodes	5
Coordinates of traffic signals	(500,0), (1000,0), (1500,0), (2000,0), (2500,0)
Vehicle start and end points	(0,0), (3000,0)
Coordinates of RSUs	(500,50), (1000,50), (1500,50), (2000,50), (2500,50)
Coordinates of cloud nodes	(1500,100)
Simulation duration	400s

B. Performance Analysis

1) Results and analysis of the whole pass-through rate evaluation of the road area: Fig. 6 illustrates the vehicle distribution when the HV (red vehicle) enters the green wave road at different times between two traffic lights. Fig. 7 presents the overall pass-through rate of the road area at the corresponding time moment. Traffic signal phases and driving conditions are reflected in the overall pass-through rate, which can provide speed recommendations for the MiGWG strategy.

(a) Time moment 0s

(b) Time moment 10s

(c) Time moment 20s

(d) Time moment 30s

(e) Time moment 40s

(f) Time moment 50s

(g) Time moment 60s

(h) Time moment 70s

(i) Time moment 80s

Fig. 6: The road scene during the simulation process.

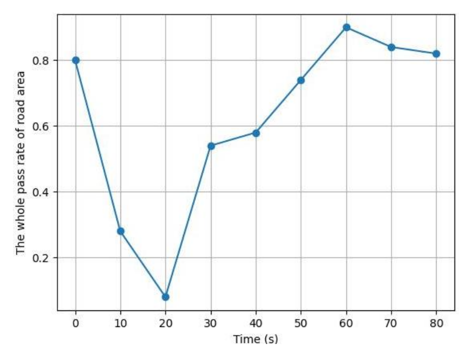

Fig. 7: The whole pass-through rate of the road area.

2) Results and analysis of the road pass-through rate: Fig. 8 illustrates the distribution of the road pass-through rate at a specific time moment.

Label ① corresponds to the scenario shown in Fig. 8(a). In Fig. 8(b), the pass-through rate in area ② is significantly lower than in adjacent grids due to the presence of trucks. Area ③ also shows a reduced rate, as trucks exert greater influence on adjacent lanes compared to sedans. In area ④, the lower

(a) Time moment 15s

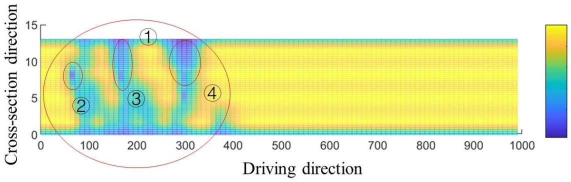

(b) Pass-through rate distribution of the road

Fig. 8: Green wave pass-through rate distribution.

rate is caused by truck overtaking and the presence of two sedans in neighboring lanes. Overall, the road pass-through rate distribution is consistent with the actual traffic conditions.

C. MiGWG Performance Analysis

1) MiGWG strategy results and analysis: Fig. 9 illustrates the guidance results of the MiGWG algorithm, compared with those obtained using the improved ACO for HV.

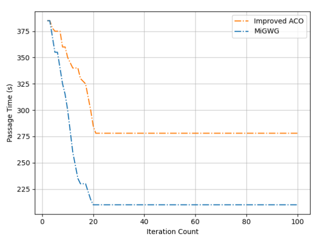

(a) Overall passage time

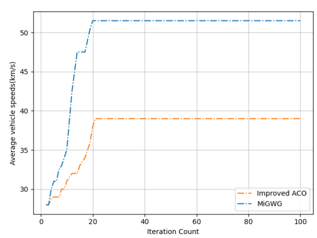

(b) Average vehicle speeds

Fig. 9: Passage time and average speed comparison.

The figures demonstrate that the MiGWG algorithm improves vehicle speed and decreases travel time.

2) Comparison experiment: A series of comparative experiments were conducted to evaluate the performance of the proposed methods. As illustrated in Fig. 10, the MiGWG algorithm effectively enhances overall traffic efficiency by improving vehicle coordination.

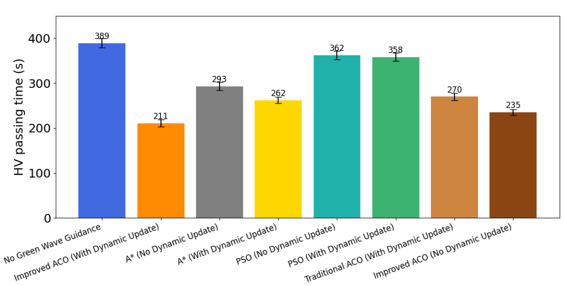

Fig. 10: HV Green Wave Passage Duration.

V. CONCLUSION

In this paper, a dynamic MiGWG strategy is proposed to help vehicles pass in a green wave. We first construct a business process for the MiGWG service based on cross-network collaboration. Next, an improved model is proposed for the evaluation of the road pass-through rate. Then, the ACO is improved based on the road pass-through rate distribution. Finally, the dynamic trajectory updating strategy is introduced to solve the impact of vehicle mobility on the real-time generation of the MiGWG strategy. The experimental results demonstrate that the proposed method effectively improves traffic efficiency and vehicle passing performance. In future work, real urban traffic data will be used for validation.

ACKNOWLEDGMENT

This work was supported by the State Key Laboratory of Intelligent Vehicle Safety Technology(IVSTSKL-202513) and the Special Key Project of Chongqing Technology Innovation and Application Development under Grant CSTB2022TIAO-STX0001.

REFERENCES

[1] Y. Zheng, R. Guo, D. Ma, Z. Zhao, and X. Li, ”A novel approach to coordinating green wave system with adaptation evolutionary strategy,” IEEE Access, vol. 8, pp. 214115-214127, 2020.

[2] W. Hao and L. Chang-ze, ”Optimization of arterial green-wave considering turning tram lines,” Journal of Traffic and Transportation Engineering, vol. 20, no. 1, pp. 204-214, 2020.

[3] B. Gao, J. Liu, H. Zou, J. Chen, L. He, and K. Li, ”Vehicle-Road-Cloud Collaborative Perception Framework and Key Technologies: A Review,” IEEE Transactions on Intelligent Transportation Systems, vol. 25, no. 12, pp. 19295-19318, 2024.

[4] Y. Yang, S. Chen, and J. Sun, ”Modeling and evaluation of speed guidance strategy in VII system,” in 13th International IEEE Conference on Intelligent Transportation Systems, 2010: IEEE, pp. 1045-1050.

[5] Q. Xu, J. Wang, B. Wang, and X. Yan, ”Modeling and simulation of intersection quasi-moving block speed guidance based on connected vehicles,” Journal of intelligent and connected vehicles, vol. 3, no. 2, pp. 67-78, 2020.

[6] L. W. Chen and C. C. Chang, ”Cooperative Traffic Control With Green Wave Coordination for Multiple Intersections Based on the Internet of Vehicles,” IEEE Transactions on Systems Man & Cybernetics Systems, pp. 1-15, 2016.

[7] Y. Shi, J. Li, Q. Han, and L. Lv, ”A Coordination Algorithm for Signalized Multi-Intersection to Maximize Green Wave Band in V2X Network,” IEEE Access, vol. 8, pp. 213706-213717, 2020.

[8] Y. Qin, D. Song, H. Chen, W. Cheng, G. Jiang, and G. J. a. p. a. Cottrell, ”A dual-stage attention-based recurrent neural network for time series prediction,” 2017.

[9] R. Jozefowicz, W. Zaremba, and I. Sutskever, “An empirical exploration of recurrent network architectures,” in Proc. 32nd Int. Conf. Machine Learning (ICML), 2015, pp. 2342–2350.

[10] W. Zhou, G. Shen, Z. Zhao, et al., “A transformer-based approach for traffic prediction with fusion spatiotemporal attention,” Knowledge-Based Systems, vol. 329, 2025.

[11] R. Robotin, G. Lazea, and C. Marcu, Graph Search Techniques for Mobile Robot Path Planning. Engineering the Future, 2010.

[12] J. Bohren et al., ”Little Ben: The Ben Franklin Racing Team’s Entry in the 2007 DARPA Urban Challenge,” Journal of Field Robotics, vol. 25, 2008.

[13] X. Xiong, H. Min, Y. Yu, and P. Wang, ”Application improvement of A* algorithm in intelligent vehicle trajectory planning,” Mathematical biosciences and engineering : MBE, vol. 18, no. 1, pp. 1-21, 2021.

[14] X.-h. Liu, D. Zhang, J. Zhang, T. Zhang, and H. Zhu, ”A path planning method based on the particle swarm optimization trained fuzzy neural network algorithm,” Cluster Computing, vol. 24, no. 3, pp. 1901-1915, 2021.

[15] Q. Han et al., ”An MEC Architecture-Oriented Improved RRT Algorithm for Regional Trajectory Planning,” Mobile Information Systems, 2021.

[16] Q. Han et al., ”The road regional hazard level evaluation method based on ising model,” in 2018 IEEE Intelligent Vehicles Symposium (IV), 2018: IEEE, pp. 1937-1942.